Acta of Bioengineering and Biomechanics
Vol. 21, No. 2, 2019

Original paper
DOI: 10.5277/ABB-01326-2019-03

Development of multi-phase models of blood flow for medium-sized vessels with stenosis

MAGDALENA KOPERNIK[1]*, PAWEŁ TOKARCZYK[1]

AGH University of Science and Technology, Krakow, Poland.

Purpose: The purpose of the work was to develop two-phase non-Newtonian blood models for medium-sized vessels with stenosis using power law and Herschel–Bulkley models. *Methods:* The blood flow was simulated in 3D models of blood vessels with 60% stenosis. The Ansys Fluent software was applied to implement the two-phase non-Newtonian blood models. In the present paper, the mixture model was selected to model the two phases of blood: plasma and red blood cells. *Results:* Simulations were carried out for four blood models: a) single-phase non-Newtonian, b) two-phase non-Newtonian, c) two-phase Herschel–Bulkley with yield stress 0 mPa, and d) two-phase Herschel–Bulkley with yield stress 10 mPa for blood plasma, while flow took place in vessel with stenosis 60%. Presentation of results in this paper shows that stenosis can substantially affect blood flow in the artery, causing variations of velocity and wall shear stress. Thus, the results in the present paper are maximum values of blood velocity and wall shear stress, profiles and distributions of blood velocity and wall shear stress computed for single- and two-phase blood models for medium-sized vessels with stenosis. *Conclusions:* For the two-phase blood models the influence of initial velocity on blood flow in the stenosis zone is not observed, the velocity profiles are symmetric and parabolic. Contrary, for the single phase non-Newtonian blood model, the velocity profile is flat in the stenosis zone and distribution of velocity is disturbed just behind the stenosis zone. The shapes of wall shear stress profiles for two-phase blood models are similar and symmetric in the center of stenosis. The biggest differences in maximum values of velocities and wall shear stress are observed between single phase non-Newtonian power law and Herschel–Bulkley blood models. The comparison of the obtained results with the literature indicates that the two-phase Herschel–Bulkley model is the most suitable for describing flow in medium-sized vessels with stenosis.

Key words: *multi-phase model, fluid dynamics, blood rheology, non-Newtonian blood model*

1. Introduction

The blood flow through arteries is important in many diseases. Vascular fluid mechanics plays a key role in the progression and development of arterial stenosis. In computational fluid-dynamics, for medium-sized vessels, the validity of the Newtonian hypothesis is not clear, especially in the stenotic case. The review of literature presented in [4], regarding computational studies in medium-sized vessels using non-Newtonian blood models, shows that it is acceptable to use power law and Herschel-Bulkley (HB) for stenotic vessels, what will be introduced in the present study. Many papers state that blood cannot be considered as a single-phase homogeneous viscous fluid, especially in the narrowing stenotic arteries [8]. Thus, the blood flow in narrowing tubes will be also represented by a two-layered model instead of one-layered model.

The purpose of the work was to develop a two-phase non-Newtonian blood models for medium-sized vessels with stenosis, using power law and Herschel–Bulkley models. The degree of stenosis was introduced on the basis of literature research [4], [9]. Simulations were carried out for four blood models: a) single-phase non-Newtonian, b) two-phase non-Newtonian, c) two-phase Herschel–Bulkley with yield stress 0 mPa, and d) two-phase Herschel–Bulkley with yield stress 10 mPa for blood plasma, while flow took place in vessel with stenosis of 60%.

* Corresponding author: Magdalena Kopernik, AGH University of Science and Technology, al. Mickiewicza 30, 30-059 Krakow, Poland. Phone: +48 (12) 617 51 26, fax: +48 (12) 617 29 21, e-mail: kopernik@agh.edu.pl

Received: February 23rd, 2019
Accepted for publication: April 24th, 2019

The Ansys Fluent software was applied to implement the two-phase non-Newtonian blood models. In the present paper, the mixture model was selected to model the two phases of blood: plasma and red blood cells. The mixture model was used to calculate non-Newtonian viscosity in the present work.

Selection of presentation of results shown in the paper is based on literature study, for example, work [3] indicates that stenosis can substantially affect blood flow in the artery, causing variations of velocity and wall shear stress. The two-phase non-Newtonian blood flow models are suggested to be used in the future in more advanced models considering, for example, thrombosis phenomenon in stenotic vessels.

2. Materials and methods

In paper [10], the basic physiological behaviour of stenosis was shown. The pressure loss across the stenosis not only depends on the severity of narrowing, but to a large extent on the magnitude of flow that goes through the artery. This pressure loss is due to viscous friction losses across the throat of the lesion, and separation losses that occur through acceleration of flow through the stenosis and the formation of eddies at the stenosis exit. Due to the combination of these effects, the pressure loss incurred by a stenosis increases quadratically with an increase in flow.

In the literature many works concern the modeling of various cases of stenosis, while there are very few works in the field of experimental measurements, and even fewer works that include model and experimental parts. It was presented in Chapter 3. The authors of the article were trying to simulate microfluidic systems, hence, they chose medium-diameter vessels with the most common stenosis as an object of interest to test the possibilities of modeling such systems, and then to go to a lower scale to take into account the phenomena that appear there. The flow behavior in the model corresponding to the medium-sized vessel with stenosis, on which also the authors of this work based the shape of vessel and flow conditions that correspond to the physiological ones [5], was presented in the paper [6].

In order to build a model of a blood vessel with stenosis, a solid model was made, for which the shape of blood vessel and the degree of stenosis was prepared based on publication [6]. Blood flow tests for vessels were performed for stenosis of 60%. The models of medium-sized blood vessel had a length of 90 mm and a section diameter of inlet was 3.5 mm [6]. Solid model was made in the Solid Works program 2019. Simulations were carried out in the Ansys program – the Fluent module 15.0, 2013. The key assumptions of the simulation models are presented below:

Inflow boundary

Mass flow boundary conditions were used in Ansys Fluent module 15.0, 2013 to provide prescribed flow rate and mass flux distribution at an inlet of vessel. Flow directions were specified as normal to the inlet boundary. For the steady flow, the mass flow rate was increased linearly with time from 0 to 1 $ml \cdot s^{-1}$ [5], [6].

Outflow boundary

Open boundary condition was used for outlet of the vessel.

Wall boundary

The rigid vessel, no-slip, no moving, the velocity of the fluid at the wall boundary was set to zero.

Fluid models

Four non-Newtonian incompressible, no mesh deformation blood models are listed below and their parameters are shown in Tables 1 and 2. Simulations were carried out for blood models: a) single-phase non-Newtonian, b) two-phase non-Newtonian, c) two-phase Herschel–Bulkley with yield stress 0 mPa, and d) two-phase Herschel–Bulkley with yield stress 10 mPa for blood plasma, while flow took place in vessel with stenosis 60%.

Analysis type

- Laminar, time steps 0.001 s for steady flow.
- Multiphase model mixture, cell zone conditions: face mixture.

Solver settings

- Hybrid solution initialization method and pressure-velocity coupling scheme.

FV (finite volume) mesh

- The simulations were carried out on FV grids with the number of tetrahedral elements equal to 523 403 and the number of nodes equal to 100 044. The FV meshes of lower densities were also tested, however mesh quality factors allowed to select the mesh with good orthogonal quality. The average computing time for each simulation was about

30 minutes (about 150 iterations) using standard PC computer (Intel Core i5 7400 3GHz, 8GB RAM). The density of the 3D FV grid is shown in Fig. 1.

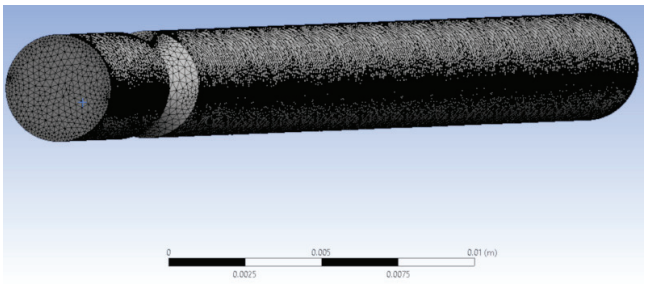

Fig. 1. 3D blood vessel model with stenosis 60% with generated FV mesh

The non-Newtonian power law blood model was used to carry out the simulations for blood considered as a single phase flow. The general power law has the form presented for example in [12], [14] as:

$$\eta = k\dot{\bar{\gamma}}^{n-1} \tag{1}$$

where: k, n – coefficients. The coefficient k represents consistency of a fluid. The larger the consistency is, the more viscous is a fluid. The coefficient n is a measure of a non-Newtonian behaviour, n = 0 represents Newtonian fluid. The closer to one this coefficient is, the more non-Newtonian are the properties of a blood. Liquids with $n > 0$ show hardening by shearing. A blood with $n < 0$ represents softening by shearing. Typical values of the coefficient in Eq. (1) for the healthy human blood set in the present work for the single phase blood model are [14]: k = 0.13 Pa and n = 0.7.

In Ansys Fluent, three different Euler–Euler multiphase models are available. In the present paper, the mixture model has been selected to model the two phases of blood: plasma and red blood cells. As in the Eulerian model, the phases are treated as interpenetrating continua. The mixture model [2] can model phases by solving the momentum, continuity, and energy equations for the mixture, the volume fraction equations for the secondary phases, and algebraic expressions for the relative velocities. The mixture model is used to calculate non-Newtonian viscosity in the present paper.

The non-Newtonian flow is modelled according to the following power law for the non-Newtonian viscosity:

$$\eta = k\dot{\bar{\gamma}}^{n-1} e^{\frac{T_0}{T}} \tag{2}$$

where: k and n have the same meaning as in the Eq. (1), and T_0 is the reference temperature.

Ansys Fluent allows to place upper and lower limits on the power law function, yielding the following equation:

$$\eta_{\min} < \eta = k\dot{\bar{\gamma}}^{n-1} e^{\frac{T_0}{T}} < \eta_{\max} \tag{3}$$

where $\eta_{\min}$ and $\eta_{\max}$ are the lower and upper limits of the power law.

If the viscosity is computed from the power law is less than $\eta_{\min}$, the value of $\eta_{\min}$ is used instead. Similarly, if the computed viscosity is greater than $\eta_{\max}$, the value of $\eta_{\max}$ is used instead. In the present work viscosity is taken from 1 to 4 mPa.

The parameters applied in computations for two-phase non-Newtonian power law blood models are presented in Table 1 [1], [11], [12].

Table 1. Parameters described in the Eq. (2) and used in the two-phase non-Newtonian power law blood model with literature references

Parameters, unit	Red blood cells	Blood plasma
Density [kg/m^3]	1090 [12]	1040 [12]
Specific heat [J/g°C]	0.87 [11]	3.93 [1]
Thermal conductivity [W/mK]	2.36 [12]	9.93 [12]
Reference temperature [K]	298 [12]	298 [12]
Consistency [mPa]	3.28 [12]	0.02 [12]
Temperature exponent [–]	0.38 [12]	0.74 [12]

The Herschel–Bulkley model [7] combines the effects of Bingham and power law behaviour in a fluid. For low strain rates, the "rigid" material acts like a very viscous fluid with viscosity μ_0. As the strain rate increases and the yield stress threshold τ_0, is passed, the fluid behaviour is described by a power law.

For $\dot{\gamma} > \dot{\gamma}_C$

$$\eta = \frac{\tau_0}{\dot{\gamma}} + k\left(\frac{\dot{\gamma}}{\dot{\gamma}_C}\right)^{(n-1)}. \tag{4}$$

For $\dot{\gamma} < \dot{\gamma}_C$

$$\eta = \tau_0 \frac{(2 - \dot{\gamma}/\dot{\gamma}_C)}{\dot{\gamma}_C} + k\left[(2-n) + (n-1)\frac{\dot{\gamma}}{\dot{\gamma}_C}\right], \tag{5}$$

where k is the consistency factor, n is the power-law index, $\dot{\gamma}_C$ is the critical shear rate, $\dot{\gamma}$ is the shear rate, τ_0, is the yield stress threshold and η is the fluid viscosity.

The Herschel–Bulkley model is commonly used to describe materials for which a constant viscosity after a critical shear stress is a reasonable assumption. In addition to the transition behavior between a flow and

no-flow regime, the Herschel–Bulkley model can also exhibit a shear-thinning or shear-thickening behavior depending on the value of n. The parameters applied in computations for two-phase Herschel–Bulkley blood model are presented in Table 2 [13].

Table 2. Parameters described in the Eq. (4) and used in the two-phase Herschel–Bulkley blood model

Parameters, unit	Red blood cells	Blood plasma
Yield stress [mPa]	15	0 and 10
Critical shear rate [s^{-1}]	1	1
Consistency [mPas]	3.28	0.02
Exponent [–]	0.38	0.74

3. Discussion

All simulations were carried out on grids, the density of which is shown in Fig. 1. where the stenosis zone is particularly visible. In the center of 60% stenosis in 3D blood vessel model, intermediate flow velocities equal to 0.8 m·s^{-1} were observed for the HB two-phase blood models, as shown in Fig. 2. The profiles of velocities for the HB two-phase blood models almost overlapped for yield stress equal to 0 and 10 mPa in the Fig. 3. The blood velocity profile for the HB model with yield stress 10 mPa and maximum velocity equal to 0.802 m·s^{-1} was located higher than the blood velocity profile for the HB model with yield stress 0 mPa and maximum velocity equal to 0.793 m·s^{-1}. The velocity profile for the two-phase non-Newtonian power law had the biggest values of blood velocities equal to 1.13 m·s^{-1} and it was a parabolic profile, as observed for the HB two-phase blood model. The single-phase non-Newtonian power law blood model had the smallest values of velocities equal to 0.724 m·s^{-1} among all analysed blood models and its velocity profile is flat in the stenosis zone.

The flatness in profiles of velocities in Fig. 2 for single phase blood model in comparison with parabolic profiles for two-phase blood models (Figs. 2 and 3) was caused by a big value of initial velocity (here 10 centimetres per second) and type of blood model. For smaller initial velocities (like micrometers per second), the velocity profiles for single phase and two-phase blood models were parabolic and symmetric. For two-phase blood models, the influence of initial velocity on blood flow velocity profiles in the stenosis zone was not observed. Thus, it can be started the two-phase blood models are more resistant to disturbances caused by initial blood flow conditions.

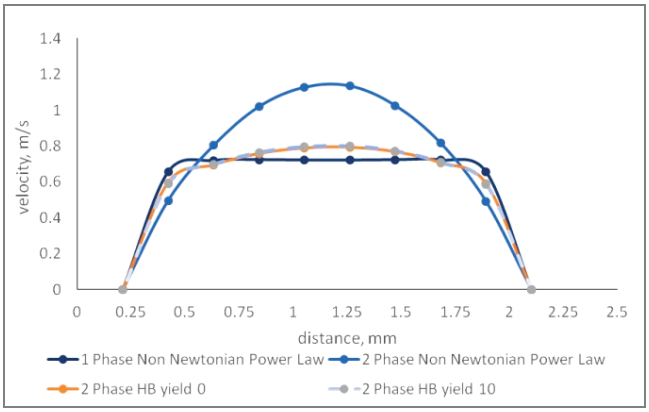

Fig. 2. Summary chart of blood velocity profiles in the center of stenosis 60% for single phase non-Newtonian power law blood model and two-phase non-Newtonian, and Herschel–Buckley blood models

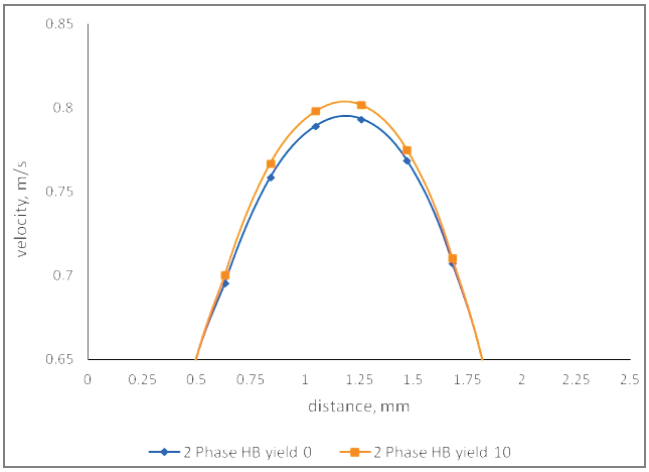

Fig. 3. Enlargement of the graph shown in Fig. 2 in the overlap zone of the blood velocity profiles in the center of stenosis 60% for two-phase Herschel–Buckley blood models

In the center of 60% stenosis in 3D blood vessel model, the biggest value of wall shear stress equal to 19.2 Pa was observed for the single phase non-Newtonian blood model, as shown in Fig. 4. The wall shear stress profile for single phase blood model was asymmetrical in the stenosis zone, in comparison with symmetric profiles of the two-phase blood models. The profiles of wall shear stress for the HB two-phase blood models almost overlapped for yield stress equal to 0 and 10 mPa, as can be seen in Fig. 5. The profile with maximum wall shear stress equal to 0.162 Pa for the HB two-phase blood model with yield stress 10 mPa is located lower than the profile with maximum wall shear stress equal to 0.172 Pa for the HB two-

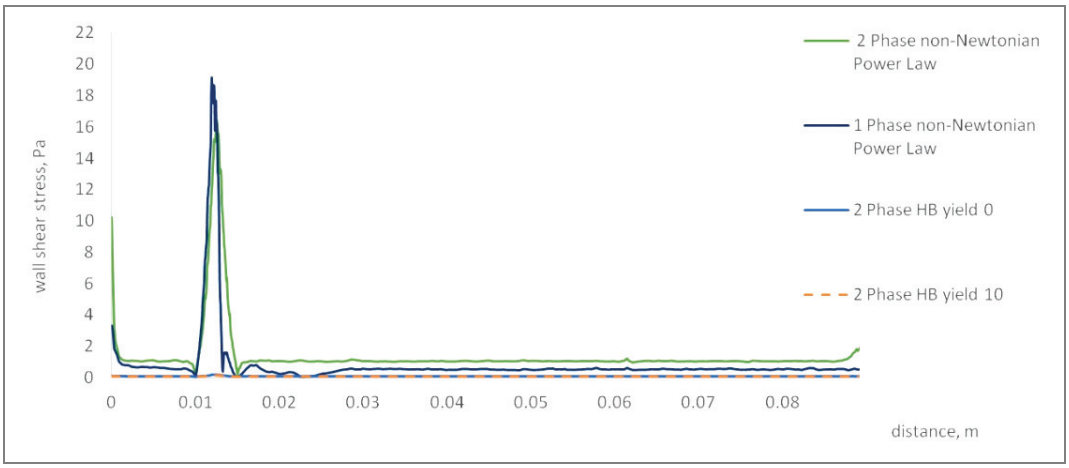

Fig. 4. Summary chart of profiles for wall shear stress in the center of stenosis 60% for single phase and two-phase blood models using non-Newtonian power law, and Herschel–Buckley

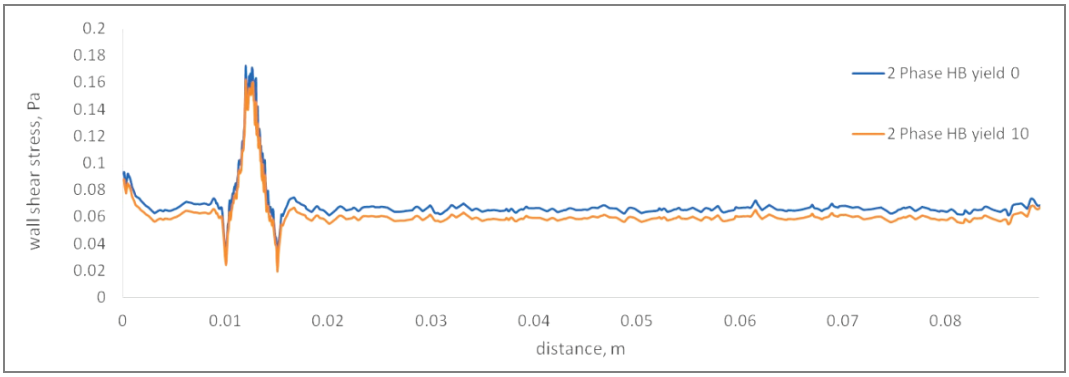

Fig. 5. Enlargement of the graph shown in Fig. 4 in the overlap zone of the blood wall shear stress profiles in the center of stenosis 60% for two-phase Herschel–Buckley blood models

phase blood model with yield stress 0 mPa. Thus, the smallest values of wall shear stress were observed for the two-phase HB blood model. The two-phase non-Newtonian blood model had intermediate values of wall shear stress equal to 16.4 Pa among all analysed blood models in the stenosis zone.

The shapes of wall shear stress profiles for two-phase blood models were similar and symmetric in the center of stenosis. In the zone before and behind the center of stenosis, the wall shear stress profiles converged to the minimum values of wall shear stress in all analysed blood models. However, these minimum values of wall shear stress behind the center of stenosis were smaller than before the center of stenosis. Contrary, the single phase model was not symmetrical and there were disturbances of wall shear stress profile in the stenosis zone and just behind it for this blood model. The velocity and wall shear stress profiles obtained in the present paper for single and two-phase blood models with vessel stenosis were similar to those presented in literature [9], [13].

The velocity distributions for two-phase blood models were homogenous in the zone before and behind the stenosis, as shown in Fig. 6. It can be concluded that the two-phase blood model was more stable and resistant to disturbances caused by a big initial velocity observed for medium-sized vessels. The distribution of blood velocity for vessel model with stenosis 60% showed increasing values in the stenosis zone for all models. The biggest blood velocity gradients occured in the zone behind the stenosis in the case of a single-phase model.

The two-phase blood models developed in this work were more stable than single phase model and will be used to build a more advanced version of blood model that takes into account the thrombosis phenomenon in a meso scale in stenotic vessels. In the future model, wall shear stress plays very important role, because if activates platelets after exceeding the critical value equal to 20 Pa. In the present work, this critical value of wall shear stress was not achieved in any of the analysed models despite of the big initial velocity observed in medium-sized vessels.

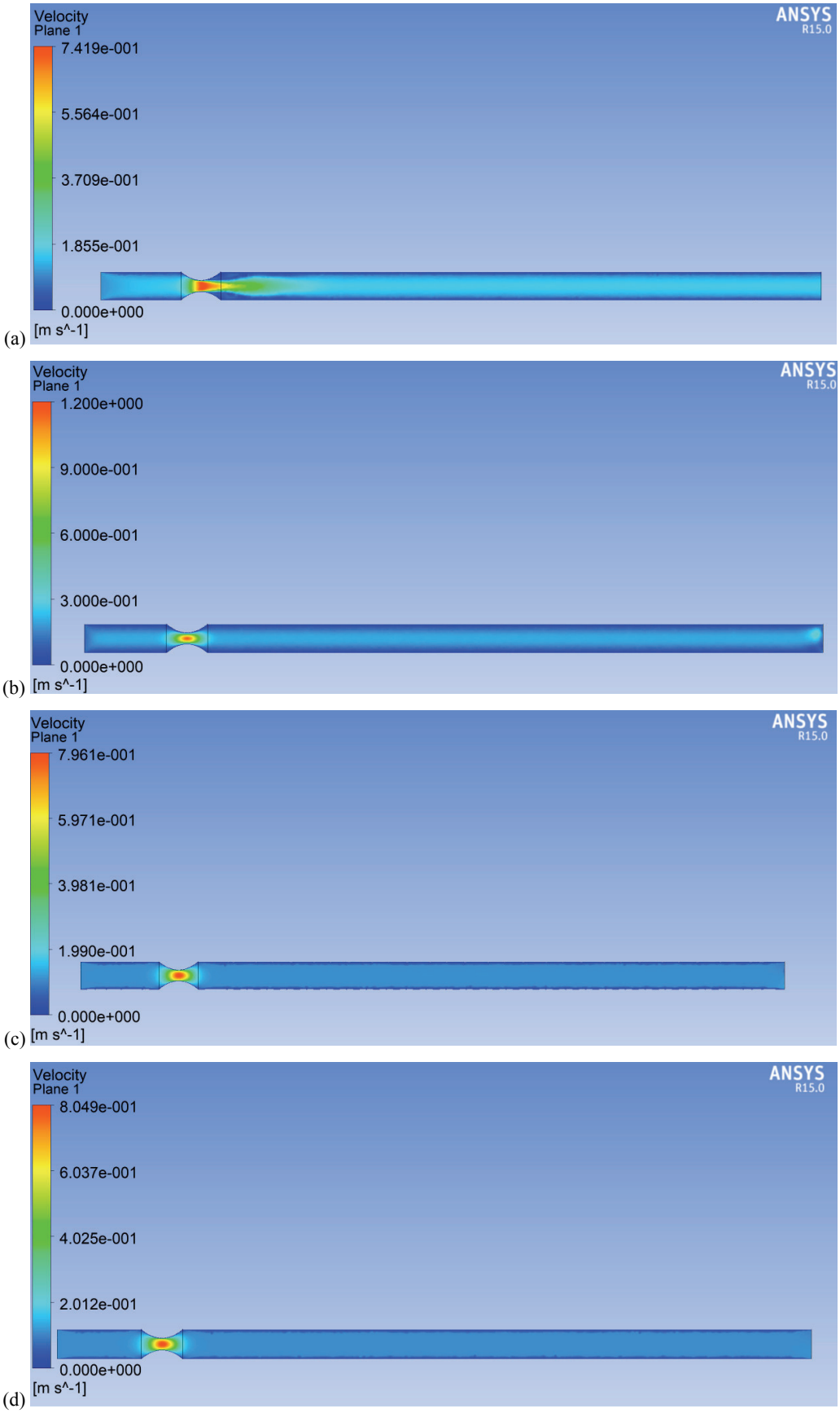

Fig. 6. Distribution of blood velocity for: (a) a non-Newtonian single-phase, (b) a non-Newtonian two-phase, (c) a two-phase Herschel–Bulkley with yield stress 0 mPa, and (d) a two-phase Herschel–Bulkley with yield stress 10 mPa blood models on entire length of the blood vessel with stenosis 60%

Medium-sized vessels of a diameter twice as big as that in this study and stenoses within the range of stenosis analyzed in this study were investigated using the PIV (particle image velocimetry) method in the paper [15] for blood considered as Newtonian and non-Newtonian fluid. Stenosis given in the model in the present paper falls within the range tested by the PIV method, although, due to the bigger diameter of the vessel and many times bigger flow rates, two times bigger velocities in the stenosis zone were obtained. The velocity distributions in the stenosis zone can be considered comparable to those obtained in this study, in experimental studies, there is a clear increase in the flow velocity in the stenosis zone, as it is in the model. The work [15] also shows the distributions of wall shear stress, which for 60% stenosis would take 1–20 Pa, which corresponds to the range of values obtained in this work for the single and two-phase non-Newtonian power law blood models. Also the maximum values of wall shear stress were obtained in the stenosis zone in the mentioned work [15].

The medium-sized vessels with a comparable diameter and length, but slightly smaller stenosis were examined by the Doppler method in work [16]. Both, the experimentally obtained flow velocity equal to $1 m \cdot s^{-1}$ in the stenosis zone and the profile of velocity in the cross-section of the vessel with stenosis correspond to the results obtained in the present paper for single-phase non-Newtonian and for two-phase HB blood models.

Besides of works dedicated only to modelling or only to experimental measurements, there are also works that combine both methods. In [4], vessels with stenosis comparable to that of the present study were analyzed and the authors showed the results of the 70's, which indicate the velocity profiles in the stenosis zone which are the most similar to these of the two-phase HB blood model from this work. In work [17], a wide analysis of stenoses and boundary conditions was carried out for numerical models of vessel with stenosis. The experimental studies in paper [17], with the use of impulse ultrasonic flowmeter, were made for stenosis 75% and a Newtonian fluid. The authors of the present work, in order to compare the results obtained from the developed rheological models, made a FV model of blood vessel with diameter 4 mm and with stenosis 75% for the flow equal to 150 ml/min, as in experiment in the paper [17]. The simulations were carried out on FV grids with the number of tetrahedral elements equal to 665 886 and the number of nodes equal to 130 008. The obtained results of the flow velocity are shown in Fig. 7 for single phase non-Newtonian power law, two-phase non-Newtonian, Herschel–Buckley blood models and experimental single phase Newtonian fluid [17]. The flow velocity measured in the experiment in the stenosis zone for the Newtonian fluid is lower than flow velocity calculated in the numerical model of vessel with stenosis 75% applying non-Newtonian blood rheological models, except for the result obtained for the two-phase HB model blood model with yield stress 0 mPa.

Presentation of results in this paper shows that stenosis can substantially affect blood flow in the artery, causing variations of velocity and wall shear stress. Thus, the results in the present paper are maximum

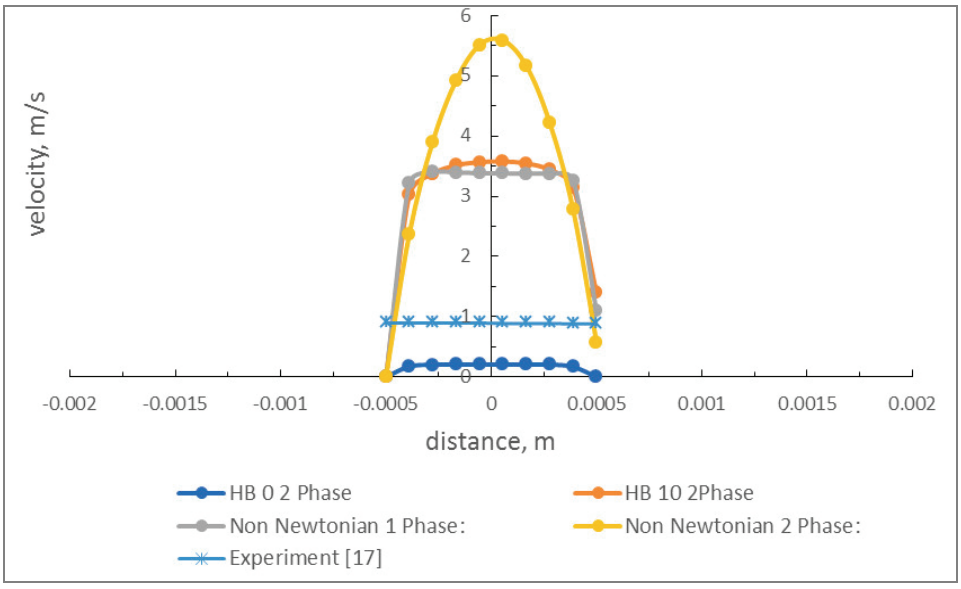

Fig. 7. Summary chart of blood velocity profiles in the center of stenosis 75% for single phase non-Newtonian power law blood model, two-phase non-Newtonian, Herschel–Buckley blood models and experimental single phase Newtonian fluid [17]

values of blood velocity and wall shear stress, profiles and distributions of blood velocity and wall shear stress computed for single and two-phase blood models for medium-sized vessels with stenosis.

Wall shear stress profiles are generated for measuring points located on the entire length of the blood vessel model. Velocity profiles are made for measuring points located on the entire width of the stenosis zone. The maximum values of velocity and wall shear stress are taken from the central point of stenosis zone. Velocity distributions are shown for the range of legends adjusted to the maximum value for a particular simulation.

4. Conclusions

For two-phase blood models the influence of initial velocity on blood flow velocity profiles in the stenosis zone is not observed, their profiles are symmetric and parabolic. On the contrary, for the single-phase non-Newtonian blood model the velocity profile is flat in the stenosis zone. Thus, the two-phase blood models are more resistant to disturbances caused by initial blood flow conditions.

The shapes of wall shear stress profiles for two-phase blood models are similar and symmetric in the center of stenosis.

The biggest differences in maximum values of wall shear stress are observed between single-phase non-Newtonian and Herschel–Bulkley blood models. The two-phase Herschel–Bulkley blood model for two yield stresses also shows differences, although these differences are very small.

The single-phase non-Newtonian blood model has the biggest values of wall shear stress and the smallest values of velocity among all analyzed blood models, as well as asymmetric profile of wall shear stress, a flat profile of velocity in the stenosis zone, and the biggest velocity gradients just behind the stenosis zone. Although, this blood model is less stable and less resistant to initial blood flow conditions.

The comparison of the obtained results with the literature indicates that the two-phase Herschel–Bulkley model is the most suitable for describing flow in medium-sized vessels with stenosis.

Acknowledgements

The work was realized as a part of fundamental research No. 16.16.110.663 financed by AGH University of Science and Technology.

References

[1] BLAKE A.S.T., PETLEY G.W., DEAKIN C.D., *Effects of changes in packed cell volume on the specific heat capacity of blood: implications for studies measuring heat exchange in extracorporeal circuits*, Brit. J. Anaesth., 2000, 84 (1), 28–32.

[2] BOWEN R.M., *Incompressible porous media models by use of the theory of mixtures*, Int. J. Eng. Sci., 1980, 18 (9), 1129–1148.

[3] CHAICHANA T., SUN Z., JEWKES J., *Hemodynamic impacts of left coronary stenosis: A patient-specific analysis*, Acta Bioeng. Biomech., 2013, 15 (3), 107–112.

[4] FENG R., XENOS M., GIRDHAR M., KANG W., DAVENPORT J.W., DENG Y., BLUESTEIN D., *Viscous flow simulation in a stenosis model using discrete particle dynamics: a comparison between DPD and CFD*, Biomech. Model Mechanobiol., 2012, 11, 119–129.

[5] HELLER L.I., SILVER K.H., VILLEGAS B.J., BALCOM S.J., WEINER B.H., *Blood flow velocity in the right coronary artery: assessment before and after angioplasty*, J. Am. Coll. Cardiol., 1994, 24(4), 1012–1017.

[6] LIN K.Y., SHIH T.C., CHOU S.H., CHEN Z.Y., HSU C.H., HO C.Y., *Computational fluid dynamics with application of different theoretical flow models for the evaluation of coronary artery stenosis on CT angiography: comparison with invasive fractional flow reserve*, Biomed. Phys. Eng. Express, 2016, 2, 065011, DOI: 10.1088/2057 1976/2/6/065011.

[7] MITSOULIS E., *Flows of viscoplastic materials: models and computations*, Rheol. Rev., 2007, 135–178.

[8] NANDA S.P., BASU MALLIK B., *A non-newtonian two-phase fluid model for blood flow through arteries under stenotic condition*, Int. J. Pharm. Bio. Sci., 2012, 2 (2), 237–247.

[9] PARK Y.R., KIM S.J., KIM S.J., KIM J.S., KANG H.S., KIM G.B., *A study on hemodynamic characteristics at the stenosed blood vessel using computational fluid dynamics simulations*, J. Biomed. Nanotechnol., 2013, 9, 1137–1145.

[10] STEGEHUIS V.E., WIJNTJENS G.W.M., MURAI T., PIEK J.J., VAN DE HOEF T.P., *Assessing the haemodynamic impact of coronary artery stenoses: intracoronary flow versus pressure measurements*, Eur. Cardiol. Rev., 2018, 13 (1), 46–53.

[11] PONDER E., *The specific heat and the heat of compression of human red cells, sickled red cells, and paracrystalline rat red cells*, J. Gen. Physiol., 1955, 38 (5), 575–580.

[12] ROSENTRATER K.A., FLORES R.A., *Physical and rheological properties of slaughterhouse swine blood and blood components*, T. ASAE, 1997, 40 (3), 683–689.

[13] SAKAR D.S., LEE U., *Influence of slip velocity in Herschel–Bulkley fluid flow between parallel plates – A mathematical study*, J. Mech. Sci. Technol., 2016, 30, 3203–3218.

[14] WALBURN F.J., SCHNECK D.J., *A constitutive equation for whole human blood*, Biorheology, 1976, 13, 201–210.

[15] DICARLO A.L., HOLDSWORTH D.W., POEPPING T.L., *Study of the effect of stenosis severity and non-Newtonian viscosity on multidirectional wall shear stress and flow disturbances in the carotid artery using particle image velocimetry*, Med. Eng. Phys., 2019, 65, 8–23.

[16] ZHANG Y., ZHANG Y., GAO L., DENG L., HU X., ZHANG K., LI H., *The variation in frequency locations in Doppler ultrasound spectra for maximum blood flow velocities in narrowed vessels*, Med. Eng. Phys., 2017, 49, 46–55.

[17] MALOTA Z., GLOWACKI J., SADOWSKI W., KOSTUR M., *Numerical analysis of the impact of flow rate, heart rate, vessel geometry, and degree of stenosis on coronary hemodynamic indices*, BMC Cardiovascular Disorders, 2018, 18(132), 1–16.